J Neurophysiol 127: 452–462, 2022.
First published January 12, 2022; doi:10.1152/jn.00081.2021

american physiological society

JNP JOURNAL OF NEUROPHYSIOLOGY

RESEARCH ARTICLE

Sensory Processing

Comparing the electrophysiological effects of traumatic noise exposure between rodents

Lenneke Kiefer,[1,2] Lisa Koch,[1] Melisa Merdan-Desik,[1,3] Bernhard H. Gaese,[1] and Manuela Nowotny[1,3]

[1]Institute of Cell Biology and Neuroscience, Goethe University, Frankfurt am Main, Germany; [2]Department of Otolaryngology at Unfallkrankenhaus Berlin (UKB), Berlin, Germany; and [3]Institute of Zoology and Evolutionary Research, Friedrich-Schiller-University, Jena, Germany

Abstract

Noise-induced hearing deficits are important health problems in the industrialized world. As the underlying physiological dysfunctions are not well understood, research in suitable animal models is urgently needed. Three rodent species (Mongolian gerbil, rat, and mouse) were studied to compare the temporal dynamics of noise-induced hearing loss after identical procedures of noise exposure. Auditory brainstem responses (ABRs) were measured before, during, and up to 8 wk after noise exposure for threshold determination and ABR waveform analysis. Trauma induction with stepwise increasing sound pressure level was interrupted by five interspersed ABR measurements. Comparing short- and long-term dynamics underlying the following noise-induced hearing loss revealed diverging time courses between the three species. Hearing loss occurred early on during noise exposure in all three rodent species at or above trauma frequency. Initial noise level (105 dB SPL) was most effective in rats whereas the delayed level increase to 115 dB SPL affected mice much stronger. Induced temporary threshold shifts in rats and mice were larger in animals with lower pretrauma ABR thresholds. The increase in activity (gain) along the auditory pathway was derived by comparing the amplitudes of short- and long-latency ABR waveform components. Directly after trauma, significant effects were found for rats (decreasing gain) and mice (increasing gain) whereas gerbils revealed high individual variability in gain changes. Taken together, our comparative study revealed pronounced species-specific differences in the development of noise-induced hearing loss and the related processing along the auditory pathway.

NEW & NOTEWORTHY We compared deficits after noise trauma in different rodents that are typically used in hearing research (Mongolian gerbil, rat, and mouse). We observed noise-induced threshold changes and alterations in the activity of processing auditory information along the ascending auditory pathway. Our results reveal pronounced differences in the characteristics of trauma-induced damage in these different rodent groups.

ABR thresholds; acoustic overstimulation; gain factor; noise trauma; peak analysis

INTRODUCTION

Hearing impairments such as deafness, sudden hearing loss, or tinnitus affect millions of people worldwide (1). As the effects of acute deafening cannot be studied in humans, several rodent species are used to investigate noise-induced hearing loss. These species include mice (e.g., see Ref. 2), rats (e.g., see Refs. 3–6), guinea pigs (7–9), hamsters (e.g., see Refs. 10 and 11), and Mongolian gerbils (e.g., see Refs. 12–14).

Each of these models has specific advantages for studying the effects of noise trauma on hearing. Nevertheless, cross-species comparability in most commonly used animal models in this field remains to be elucidated. By performing this comparative study, we aimed to determine and characterize species-specific differences in physiological responses to noise-induced hearing damage and the recovery of hearing. Therefore, we exposed gerbils, rats, and mice to the same noise trauma and measured brainstem potentials under the same experimental conditions. This approach revealed differences in the time course of the threshold shift and recovery as well as differences in the auditory brainstem response (ABR) amplitude following exposure to high-level sound stimuli.

An efficient and reliable method to objectively investigate trauma-induced changes in hearing ability is the measurement

Correspondence: M. Nowotny (manuela.nowotny@uni-jena.de).
Submitted 19 February 2021 / Revised 17 December 2021 / Accepted 19 December 2021

of ABRs. ABRs generate a species-typical waveform pattern with a sequence of peaks and troughs (15, 16) in a temporal sequence along the auditory pathway. The short latency of *wave I* is derived from the sum of neuronal activity in the ear, including the auditory nerve (17), and long latency of *waves IV* and *V*, which are usually difficult to separate, originate from the lateral lemniscus and the inferior colliculus (18). By comparing early and late ABR waveform components at suprathreshold stimulus levels, a reference factor (gain value) can be calculated. This gain value compares response amplitudes between inputs from the ear (early response) and brainstem activity (late response). Thus, it provides insights into noise-induced changes along the auditory pathway.

Acoustic overstimulation is known to damage cellular structures in the ear important for signal transduction, such as hair bundles of sensory cells and synaptic connections (19). This damage results in a temporary or permanent reduction in hearing sensitivity, presumably involving outer hair cells (e.g., see Ref. 20). In addition, several studies identified a specific loss of synaptic connections after acoustic overstimulation known as synaptopathy (2, 8, 21, 22). Since reduced responsiveness at high sound pressure levels does not exclusively affect the commonly determined hearing threshold, the phenomenon is termed hidden hearing loss (HHL) (23, 24). ABR hearing thresholds often return to pre-noise values within several days or up to a few weeks after trauma (e.g., see Refs. 6, 8, 25, and 26). In addition to hair cell recovery (e.g., see Ref. 2), this restoration is mainly related to the re-establishment of synaptic connections involved in low sound pressure level (SPL) processing (23). In contrast, recovery of processing at high SPL is often incomplete (23, 24), and demyelination of the respective auditory nerve fibers occurs (27). Animals with fully recovered ABR thresholds that suggest normal hearing abilities could therefore have profound HHL (24, 28, 29). This damage was indicated by reduced early peak amplitudes in the ABR response to high-intensity stimulation (e.g., see Refs. 13 and 23), which mainly originates from the auditory nerve (30). A recent study on hearing in the presence of background noise in mice treated with ouabain (destroys type-I spiral ganglion cells) suggested that a combination of the loss of afferent coding together with central dysfunction produced HHL (31).

The mice used for comparison in this study were from strain C57BL/6, which is increasingly used to study hearing pathologies at the neuronal level (e.g., see Ref. 32). This strain is known for its early onset age-related hearing loss (33), as it develops progressive high-frequency hearing loss (34–38) starting approximately at the age of 3 mo, with a threshold deterioration of 20–30 dB occurring after 6 mo (38). Although C57BL/6 mice show greater hearing loss after noise exposure (39, 40), we observed threshold shifts and recovery comparable with those of the other two species investigated.

MATERIALS AND METHODS

Subjects

Data were collected from groups of three different rodent species: Mongolian gerbils, rats, and mice. All animals were housed in small groups, with males separated from females, on a light-dark cycle of 12:12 h with food and water accessible ad libitum. Measurements started in the activity period of animals (gerbils in the morning and rats in the evening) and were recorded from four different groups of rodents as follows:

1) Mongolian gerbils (*Meriones unguiculatus*): $n = 10$, males ($n = 6$) and females ($n = 4$). Average weight at the beginning of experiments: 58.2 ± 9.2 g (age: 24 ± 5 wk).

2) Laboratory rats (*Rattus norvegicus*, strain Sprague Dawley): $n = 10$, females. Average weight: 245 ± 16 g (age: 15 ± 2 wk).For mice, two different groups were used: one group with the same noise trauma as gerbils and rats, named "t8-group" (trauma centered at 8 kHz) and a second group named "t16-group" (trauma centered at 16 kHz):

3) Laboratory mice "t8-group" (*Mus musculus*, strain C57BL/6): $n = 10$, females. Average weight: 20.5 ± 1.4 g (age: 13 ± 1 wk). Acoustic trauma in this group was induced at 8 kHz, identical to gerbils and rats.

4) Laboratory mice "t16-group" (*Mus musculus*, strain C57BL/6): $n = 8$, males ($n = 4$) and females ($n = 4$). Average weight: 21.6 ± 2.4 g (age: 9 ± 1 wk). Acoustic trauma in this group was induced at 16 kHz (instead of 8 kHz for the three other groups).

In all animal groups, acoustic trauma was applied during the species-specific activity phase. Testing in mice, however, started in the early morning at the end of their activity phase (41). This process should not affect ABR measurements, since C57BL/6 mice show weak chronotolerance to short noise impulses (42).

The menstrual cycle in female animals was not monitored. All data were pooled and not handled separately for different sexes since the group size was too small for the given effect size to observe differences. Nevertheless, data points from individual animals shown in figures were labeled in different colors to indicate their sex. Experimental procedures followed federal regulations (approved by Regierungspraesidium Darmstadt, No. F104/53).

General Anesthesia

This study was designed to compare the effects of acoustic overstimulation between the three rodent species. Therefore, the experimental conditions were maintained as comparable as possible. For ABR measurements and acoustic overstimulation, all animals were anesthetized with a mixture of ketamine (Ketavet, Pfizer 100 mg/mL) and xylazine (Rompun, Bayer, 2%) diluted in physiological saline solution as needed. The initial dose (applied intraperitoneally; given per kg body weight) administered to gerbils was 112.5 mg/kg ketamine and 5 mg/kg xylazine and administered to rats was 92 mg/kg ketamine and 3.7 mg/kg xylazine. Anesthesia administered to both groups of mice was comparable with that administered to gerbils: 110 mg/kg ketamine and 11 mg/kg xylazine. The depth of anesthesia was controlled by monitoring the toe-pinch reflex and vibrissa movements. Supplemental doses were applied via continuous infusion using a micropump (Sp100i syringe pump, World Precision Instruments, Sarasota, FL). For mice, the micropump was used for the continuous infusion of Ketavet in saline only. Animals were placed on a heating pad, and body temperature was maintained at 37.5°C–38.5°C.

ABR Recordings

We performed ABR measurements using test frequencies at and around the noise trauma frequency to obtain information about the sensitivity of the auditory system at levels of the auditory nerve up to the inferior colliculus. ABR thresholds were determined using increasing sound pressure levels ranging from 0 to 80 dB SPL (step size 5 dB); in a few cases, sound pressure levels up to 90 dB SPL were applied, if necessary. Test frequencies of pure tones (10-ms duration, alternating polarity) were usually applied at 2, 8, and 14 kHz. In the t16 group of mice, however, 8, 16, and 32 kHz were tested. Stimuli were generated by an internal sound card (Juli@24-bit/192 kHz, ESI, Leonberg, Germany; in some experiments DAP 3000 A-212) controlled by a custom-built computer program written in MATLAB (The MathWorks, Inc.; v. 2007 b, Natick, MA). Signals were amplified (RB 1510, Rotel, North Reading, MA) and broadcast via a loudspeaker (MHT 12–8 Ω, Visaton, Haan, Germany) located 10 cm from the animal's left ear. ABRs were recorded differentially (Cornerstone, Ex1 with 4002 headstage, Dagan Corporation; gain = 2,000, filter 0.3–2 kHz) from subcutaneous silver wire electrodes: one at the vertex above the right inferior colliculus (+), one behind the left auditory bulla (−), and a ground electrode near the subject's tail root. ABR responses were recorded via a soundcard (96 kHz sampling rate) and averaged across 400 stimulus repetitions (interstimulus interval of 100 ms). ABR responses (Fig. 1) are typically measurements that relate neuronal activity from contralateral sides, dominated by late responses and not *peak I* (17). ABR threshold values were determined through visual inspection. An additional inspection by a second independent observer showed that thresholds differed in some cases by no more than 5 dB. For consistency, data evaluated by the first observer were used.

Acoustic Trauma

Acoustic trauma was induced by binaural noise overstimulation around a center frequency of 8 kHz (±0.25 octave noise band in three groups: gerbils, rats, and "t8-group" of mice). An additional group of mice (named the "t16-group") received noise overstimulation at 16 kHz (±0.25 oct). The acoustic signal was produced by a signal processor (RP2.1 processor, Tucker-Davis Technologies), attenuated (programmable attenuator PA5, TDT), amplified (RB 1510, Rotel, North Reading, MA), and presented free-field (20 cm above the animal) via a horn speaker (HTH 8.7, Visaton, Haan, Germany). The trauma-inducing noise (total duration of 120 min) had an initial sound pressure level of 105 dB SPL (peak-to-peak), which was increased to 115 dB SPL after 90 min of trauma, for the last 30 min. The sound presentation was interrupted five times to measure ABRs (see Fig. 2) with an interruption time of ~18 min each.

ABR Gain Analysis

ABR gain was analyzed using a custom-made program written in MATLAB (The MathWorks, Inc.; v. 2007b, Natick, MA) based on peak-to-trough amplitudes of individual ABR components at the 80 dB SPL stimulus level. For each animal, we selected an early peak (peak: vertex positive) at a latency of ~1 ms (see Fig. 1*A*) and a late peak at a latency of

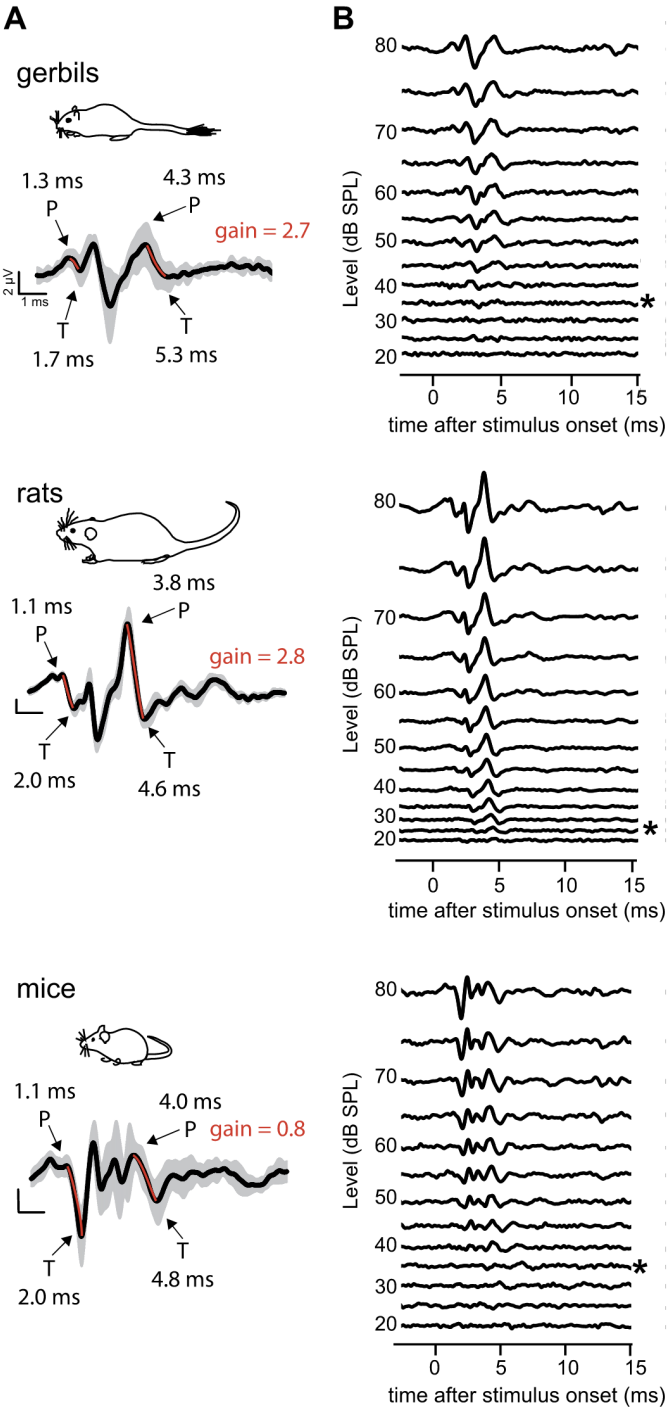

Figure 1. Auditory brainstem response (ABR) waveform characteristics and threshold detection in three rodent species. *A*: average ABR waveforms (± standard deviation shown as gray shadows; $n = 10$ for each group) at 8 kHz and 80 dB sound pressure level (SPL) in gerbils (*top*), rats (*middle*), and mice (*bottom*). Peak-to-peak amplitudes were determined from peaks (P, local maxima) and subsequent troughs (T) for early (~1 ms) and late (~4 ms) responses. We calculated the increase in neuronal activity gain along the auditory pathway by dividing the late peak-to-trough amplitude by the corresponding peak-to-trough amplitude of early components for each tested animal (red lines). *B*: exemplary averaged ABR waveforms measured at 8 kHz for sound pressure levels ranging from 20 to 80 dB SPL in 5 dB steps (each group: $n = 2$). *The species-specific thresholds (ABR at the lowest level with a clear response) in each plot.

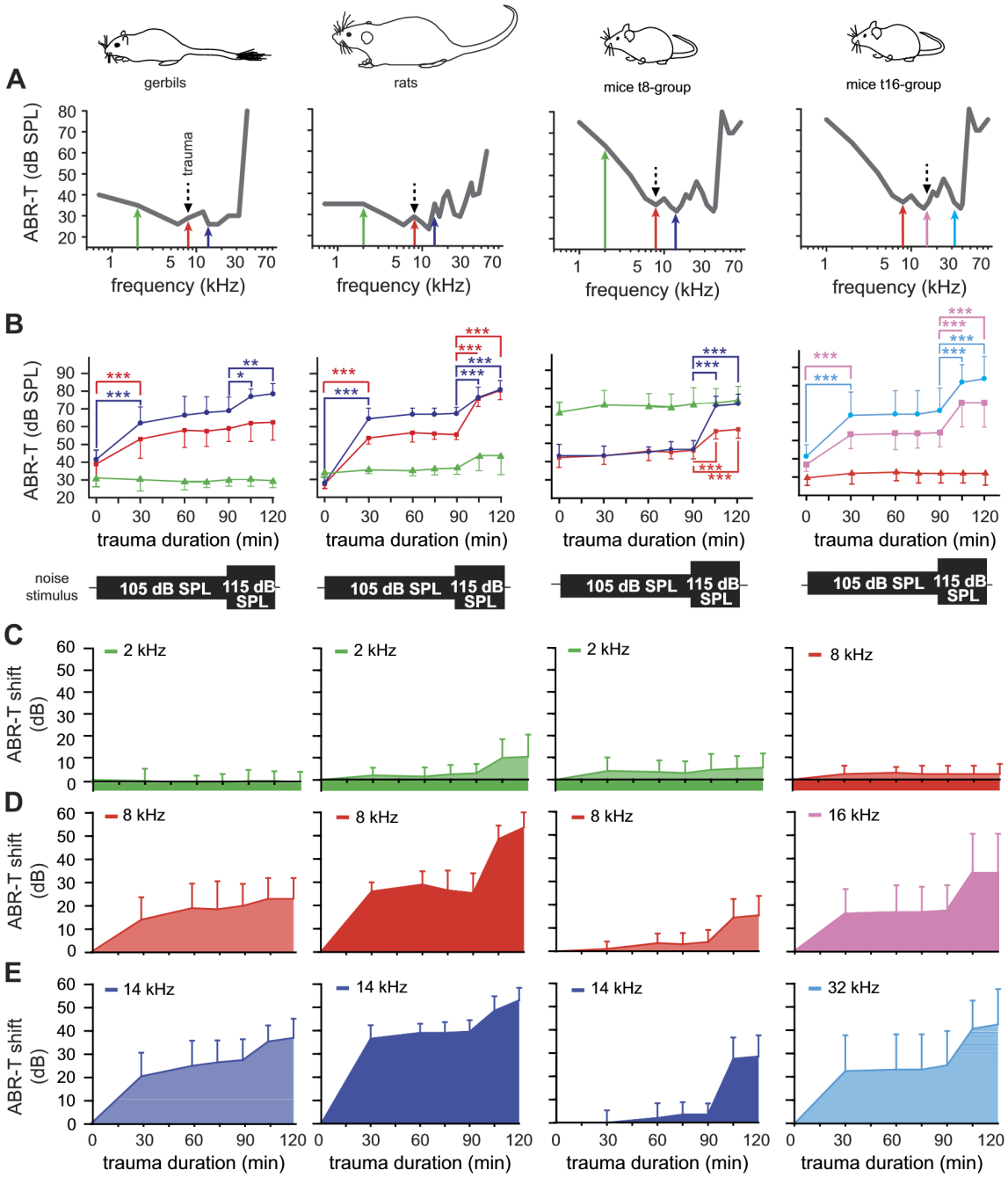

Figure 2. Time course of changes in auditory brainstem response (ABR) thresholds in three rodent species measured with stepwise noise trauma. *A*: exemplary ABR hearing thresholds (ABR-T) in three rodent species before noise trauma. The black dashed line arrow indicates the center frequency of the applied noise trauma (t8 = 8 kHz, t16 = 16 kHz). Colored arrows indicate the three test frequencies for which the time courses of ABR thresholds are shown in *B*–*E*. *B*: time course of ABR thresholds recorded in three rodent species during extended noise trauma with increasing sound pressure level (SPL). The curves for threshold development at 2 kHz (green lines), 8 kHz (red lines), and 14 kHz (blue lines) are shown. Measured frequencies differed in the t16-group of mice: 8 kHz (red lines), 16 kHz (pink lines), and 32 kHz (light blue lines). Tick intervals on the *x*-axis represent 15 min. The trauma SPL of 105 dB was further increased to 115 dB SPL at 90 min after trauma onset. The total trauma duration was 120 min. *Significant changes in thresholds over time for a particular species and frequency. Shifts in the ABR threshold (compared with pretrauma measurements) over the time course of 120 min noise trauma measured at frequencies below trauma (*C*), at the trauma center frequency (*D*), and at a higher frequency (*E*). The group size was $n = 10$ animals; the t16-group of mice, however, included $n = 8$ animals.

~4 ms. ABR gain along the auditory pathway was calculated by dividing late peak amplitude by the corresponding early peak amplitude. Gain values were averaged by group (gerbil, rat, mouse-t8, and mouse-t16). Changes in group gain values were determined based on the slope of a linear regression equation relating gain values before and after certain time points during noise trauma. Possible trauma-induced changes in processing effectiveness might become obvious using this approach.

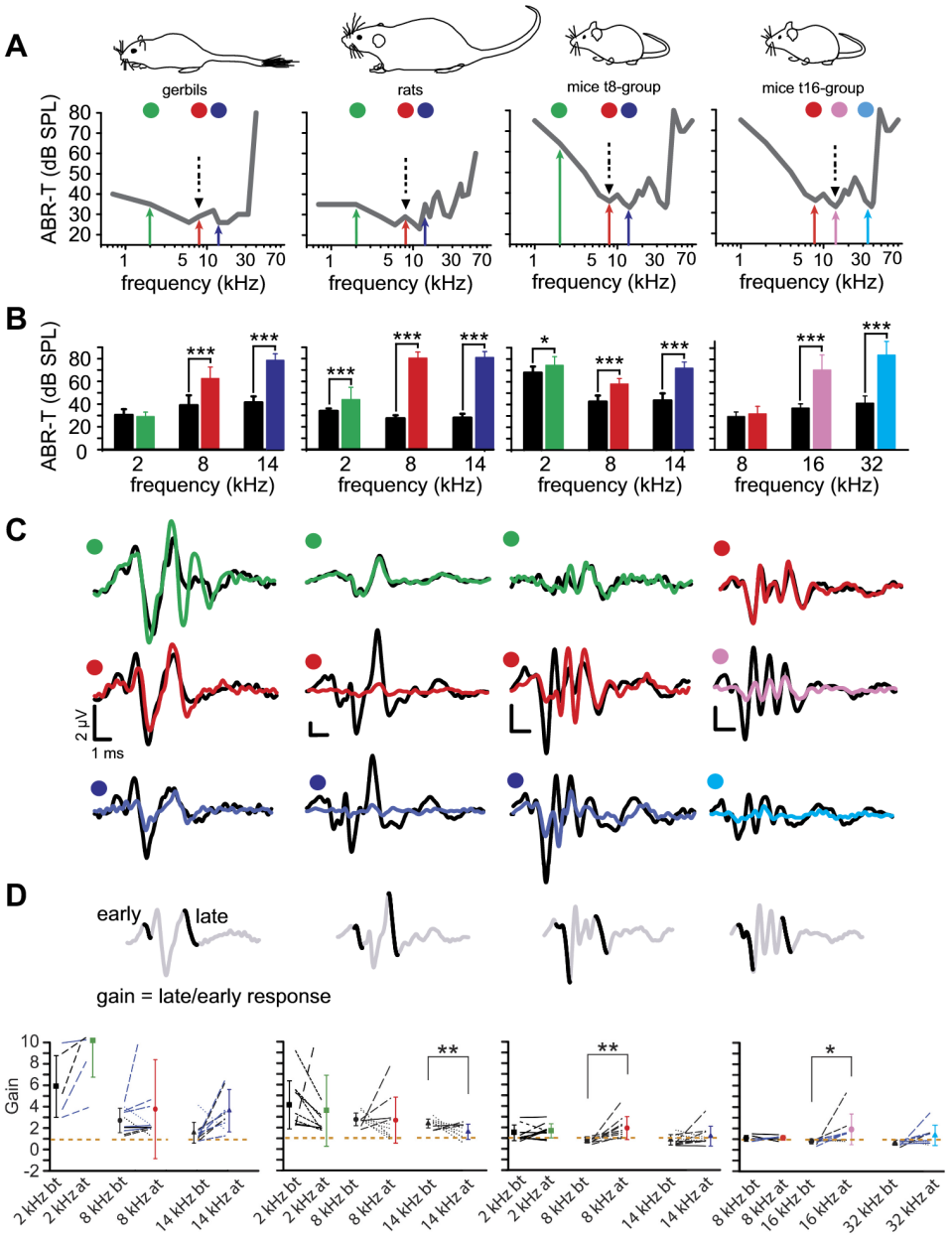

Figure 3. Detailed description of changes in auditory brainstem response (ABR) components directly after noise trauma in gerbils, rats, and mice. *A*: the four different test groups are defined by rodent species and trauma frequency (i.e., two mouse groups). The black dashed line arrow indicates the center frequency of the applied noise trauma in the exemplary measured ABR hearing thresholds (ABR-T). Colored dots and arrows indicate test frequencies (same as in Fig. 2*A*). The middle point and arrows always correspond to the center frequency of the noise trauma (8 or 16 kHz, depending on the test group). *B*: level of ABR thresholds before (black bars) and directly after (colored bars) noise trauma measured at three different test frequencies in each of the four test groups. ABR thresholds were determined at test frequencies of 2 kHz (green bar), 8 kHz (red bar), and 14 kHz (dark blue bar). An additional group of mice (t16-group of mice) were subjected to noise trauma at 16 kHz (pink bar); therefore, ABR thresholds were determined at test frequencies up to 32 kHz (light blue bar). *C*: average ABR waveforms measured at the 80 dB sound pressure level (SPL) stimulus level in all four test groups, always comparing waveforms before (black line) and directly after trauma (colored line as in *B*). These comparisons are shown for the three different test frequencies (in each column as indicated by coloring, *top* to *bottom*: low to high test frequency), always at the same stimulus level of 80 dB SPL. Note the differences in calibration (as indicated by different lengths of calibration bars) along the ordinate. *D*: noise-induced changes in amplitude gain at the 80 dB SPL stimulus level along the auditory pathway, i.e., between early and late ABR response peak components (gain = late amplitude/early amplitude). The early peak components at ~1.2 ms and the late peak components at ~4 ms latency (black sections in waveform) were used for the detailed gain analysis. Lines indicate changes in gain in individual animals at two different test frequencies per group (as indicated) before trauma (bt) and after trauma (at). Direction of trauma-related changes in gain are indicated by the line type (increase: dashed line, stable/no change: solid line, decrease: dotted line). Data from males (gerbil and t16-group of mice) are shown in blue, and data from females are shown in black. Significant changes in gain (average) are indicated above each set of lines. Black and colored dots (with error bars) indicate average gain before and after trauma, respectively. The horizontal dashed line indicates a gain of 1, i.e. equal amplitude of early and late ABR components. Significant changes in thresholds over time for a particular species and frequency are indicated by $*P < 0.05$, $**P < 0.01$ and $***P < 0.001$.

Statistical Analysis

Statistical analyses were performed with JMP software (v. 7.0; SAS Institute Inc., Cary, NC). ABR measurements were analyzed using repeated-measure ANOVAs testing the effects of frequency, time point of measurement, and animal group. Greenhouse–Geisser-corrected P values for the ABR measurements were used to minimize the error (if necessary, according to Mauchly's sphericity test). Permanent ABR changes were evaluated by performing post hoc comparisons between different time points for a particular frequency as independent contrasts corrected for multiple comparisons (Bonferroni–Holm procedure). In addition, Pearson's correlation coefficients were calculated, and pairwise comparisons were conducted using Wilcoxon's MPSR test. Significance was assumed at $P < 0.05$, and different levels of significance are marked in figures as $*P < 0.05$, $**P < 0.01$, and $***P < 0.001$.

RESULTS

We measured ABRs in gerbils, rats, and mice at different frequencies and detected noise trauma-induced changes in ABR thresholds and waveforms. Indications for different mechanisms of trauma induction were revealed through a paradigm with increasing trauma intensity during the 2-h noise application combined with repeated ABR measurements during that period. Furthermore, permanent changes in the ABRs were evaluated 8 wk after noise exposure.

General ABR Waveforms in Gerbils, Rats, and Mice

ABR waveforms result from sound-induced synchronized activity of neuronal populations at different levels along the auditory pathway that can be used to determine individual hearing thresholds. A temporal sequence of several peaks and troughs was observed in the ABR waveforms recorded from all rodent species investigated (Fig. 1*A*). Peaks were vertex-positive, i.e., neuronal responses measured near the left auditory bulla, close to the stimulated ear, were subtracted from responses measured above the right inferior colliculus. The peak amplitude and latency depended on stimulus characteristics such as the sound pressure level and frequency (Fig. 1*B*). The average ABR waveform across all animals tested (n = 38) showed a first maximum at 1.2 ± 0.3 ms after stimulus onset followed by a trough at 1.9 ± 0.2 ms (latencies measured from stimulus onset of a tone with a frequency of 8 kHz at a level of 80 dB SPL). This early response component is presumably generated by neuronal activity in the inner ear, mainly from axons or cell bodies of activated auditory nerve fibers (43). The late peak in the ABR response at 4.0 ± 0.3 ms followed by a trough at 4.9 ± 0.5 ms after stimulus onset, on the other hand, was presumably related to neuronal activity in the upper brainstem, such as the lateral lemniscus or inferior colliculus.

The Largest Shifts in the ABR Threshold Occur during the First 30 min of Noise Trauma

The same noise trauma was applied at 8 kHz (±0.25 oct) for 2 h in all three species. This trauma frequency is located in the lower third of the frequency range with high sensitivity in all three species, i.e., low hearing threshold (Fig. 2*A*). In the t8-group mice, this trauma frequency was similar to the increasing threshold at the low-frequency end of the hearing range. The sound pressure level of the trauma-inducing noise was 105 dB SPL during the first 90 min, followed by 30 min of 115 dB SPL. We determined the time course of ABR threshold shifts by interrupting the noise application every 30 min for the first hour and for the last 15 min to measure ABRs at three frequencies of 2, 8, and 14 kHz (Fig. 2*B*). In gerbils and rats, the largest and most significant shifts in ABR thresholds were observed after the first 30 min, both at the noise center frequency of 8 kHz as well as at 14 kHz. The threshold shift induced by 105 dB SPL noise was always larger at the highest test frequency (14 kHz in rats and gerbils and 32 kHz in the t16-group of mice). Thresholds plateaued at ~56 ± 6 dB SPL (gerbils and rats) at a frequency of 8 kHz and at ~67 ± 9 dB SPL at a frequency of 14 kHz. An increase in the trauma noise level by 10 dB after 90 min again led to a significant shift in the ABR threshold at 8 kHz only in rats and at 14 kHz in both groups. The total threshold shift after 120 min of noise trauma was highest in rats, with 53 ± 7 dB and 53 ± 5 dB shifts observed at 8 and 14 kHz, respectively. This effective noise trauma in gerbils and rats centered at 8 kHz with a level of 105 dB SPL was unexpectedly not appropriate to induce a significant ABR threshold shift in the t8-group of mice (Fig. 2, *D* and *E*). Only the late increase to a level of 115 dB SPL led to a clear increase in the ABR threshold. Therefore, we repeated measurements in the additional t16-group of mice (n = 8) by applying noise trauma centered at the higher frequency of 16 kHz (±0.25 oct). This trauma frequency fits slightly better to the hearing range of mice and induced a pattern of threshold shifts comparable with those in gerbils and rats. At 8 kHz, which was below the center of the noise trauma, no threshold shift was detected. ABR thresholds measured at 16 and 32 kHz were significantly higher after 30 min, followed by a threshold stable period. An increase in the trauma noise level by 10 dB (after 90 min) led to a second significant increase in the threshold at both frequencies (Fig. 2*B*, *right* column).

Trauma-Dependent Changes in the ABR Waveform Differ between Rodent Species

Significantly increased ABR thresholds at the trauma center frequency and at 14 kHz were observed in all groups immediately after the end (120 min) of acoustic overstimulation (Fig. 3, *A* and *B*). At 2 kHz, however, a significant increase in the ABR threshold was noticed in rats and mice (only the t8-group). In the additional t16-group of mice exposed to a noise trauma frequency of 16 kHz (in this case low test frequency at 8 kHz and high test frequency at 32 kHz), ABR thresholds at a frequency of 8 kHz (i.e., below noise trauma) were not affected (Fig. 3*B*).

Species-specific changes in the amplitude of individual ABR waveform components were analyzed in the three rodent groups exposed to 8 kHz noise trauma by comparing waveforms obtained at 80 dB SPL stimulation before and directly after trauma. For the early (low latency) ABR wave component, a decrease in amplitude was detected at the trauma center frequency (Fig. 3*C*, *middle* panel with black lines as ABR wave before trauma and red lines 120 min after

noise trauma) and at test frequencies above this frequency (Fig. 3*C*, *bottom* panel with black and blue lines). This finding was consistent across rodent species and (in the t16-group of mice) across trauma frequencies. Major differences, however, were observed for the late ABR waveform component. A substantial greater than 80% decrease in the amplitude of the late response was detected only in rats. In contrast, an ~20% increase in this amplitude was found in gerbils and the t8-group of mice at the trauma frequency directly after trauma.

Increase in the Amplitude Gain of Neural Activity along the Auditory Pathway is Differentially Affected by Noise Trauma in the Three Rodent Species

The change in stimulus-related activity along the auditory pathway can be estimated from the amplitudes of different ABR peak components. Determining trauma-related changes in these gain values might indicate the detailed nature of the underlying neuronal changes after noise trauma. Although short-latency "early" components represent peripheral activation (latencies of ~1.2 ms in Fig. 1*A*), stimulus-elicited activity in the upper brainstem is represented by the "late" component at a latency of ~4 ms (Fig. 1*A*). Before noise trauma, the average ABR waveforms at 2 kHz had a calculated gain (=late amplitude/early amplitude) ranging from 1.5 to 6.0 (gerbils: 6.0; rats: 4.1; mice: 1.5) that was not significantly different after noise trauma (gerbils: 10.2; rats: 3.6; mice: 1.7). At a stimulus frequency of 8 kHz (as shown in Fig. 1*A*), the calculated gains in gerbils, rats, and mice were 2.7, 2.8, and 0.8, respectively. Species-specific differences in ABR gain along the auditory pathway were already observed in pretrauma ABR waveforms. Gerbils showed positive gain factors ranging from 2.7 (±1.1 at 8 kHz) to 1.6 (±1.0 at 14 kHz; see Fig. 3*D*). Further analysis revealed a high individual variability in ABR response patterns after noise trauma in gerbils, resulting in a mixture of increasing and decreasing gain factors. The increase in amplitude gain was not significantly influenced by noise trauma (average gain after trauma; 3.8 ± 4.6 and 3.6 ± 2.0 at 8 and 14 kHz, respectively). Rats showed gain factors comparable with gerbils before trauma (8 kHz: 2.8 ± 0.6; 14 kHz: 2.4 ± 0.4). Even with dramatically decreasing ABR amplitudes after trauma, the gain between the early and late response was stable at 8 kHz (2.7 ± 2.2). This trend, however, was different at 14 kHz: the average gains significantly decreased after trauma to 1.6 ± 0.7. Mice in the t8-group generally presented lower gain factors of 0.8 (±0.2 at 8 kHz) or 0.8 (±0.5 at 14 kHz), similar to mice in the t16-group (0.8 ± 0.2 at 16 kHz and 0.7 ± 0.2 at 32 kHz). After noise trauma, at least at approximate trauma frequencies (8 kHz or 16 kHz), a significant increase in the gain to 1.9 ± 1.1 and 1.9 ± 1.4, respectively, was observed. The strength of the change in individual gain values, which was characterized by the individual gain slope before and after noise trauma, was not equal at the trauma center frequency and the frequency higher than the trauma frequency (Fig. 3*D*). A comparison of differences in gain values at 2 kHz revealed no differences before and directly after noise trauma in all rodents (data not shown).

The Total Shift of the ABR Threshold after Noise Trauma Depends on the Hearing Threshold before Noise Trauma

As pretrauma ABR thresholds varied considerably between animals in each rodent group, we tested whether individuals with more sensitive hearing (as detected by the ABR hearing threshold) were more susceptible to noise trauma. This sensitivity might lead to differences in trauma-related changes in the threshold and gain. Overall, we did not observe a strong relationship between individual hearing sensitivity before noise trauma and the gain at 8 kHz ($r = -0.42$) when all data were pooled. Regarding the different groups, only rats showed a tendency ($r = -0.61$, Fig. 4*A*) toward a correlation between a lower hearing threshold and a higher gain. However, individual threshold shifts (directly after trauma) were negatively correlated with ABR threshold levels before trauma (Fig. 4*B*). A correlation of the ABR threshold values before noise trauma and the acute threshold shift values directly after trauma revealed a significant correlation in

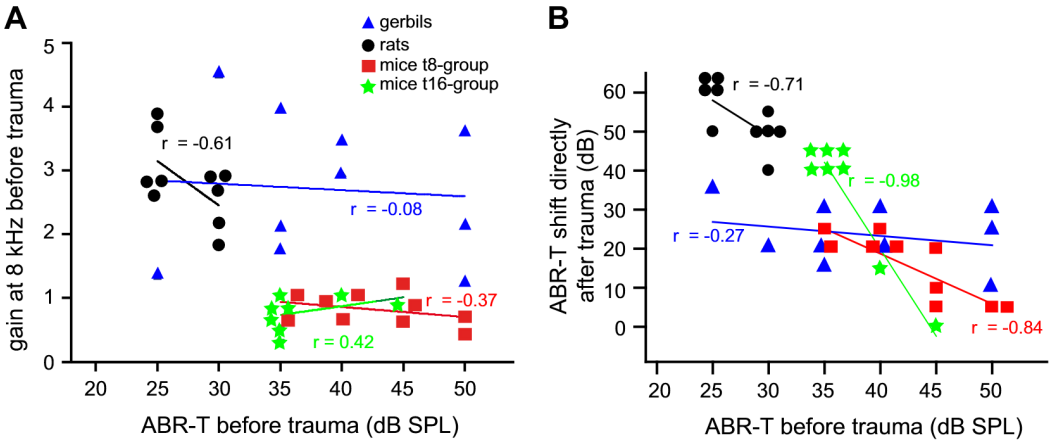

Figure 4. Individual auditory brainstem response (ABR) threshold correlation. *A*: correlation of individual gain values measured at 80 dB sound pressure level (SPL) and ABR hearing thresholds (ABR-T) at the 8 kHz baseline. Individual data from gerbils ($n = 10$, blue triangles), rats ($n = 10$, black circles), and mice (t8-group of mice, $n = 10$, red squares and t16-group of mice, $n = 8$, green stars) were fitted by group to a linear regression model. *B*: correlation between noise-induced threshold shifts and ABR thresholds before noise application. For all animal groups, linear regression curves were calculated to fit the data.

mice (t8-group: $r = -0.84$, $P < 0.0026$; t16-group: $r = -0.98$, $P = 0.0001$) and rats ($r = -0.71$, $P = 0.0216$). This correlation of the ABR threshold before and directly after noise trauma was also identified when the groups of rats and mice were pooled ($r = -0.93$, $P < 0.001$). In these groups, animals with a lower ABR threshold before noise trauma showed a greater increase in the threshold within the first 2 h after noise trauma. Only gerbils showed substantial variability in ABR threshold values before noise trauma that were not significantly correlated with shifts in the ABR threshold directly after noise trauma. All tested animals had a stable noise-induced threshold shift of ~24 dB. This finding suggests a general limit for the trauma-induced threshold shift in the peripheral auditory system.

Recovery after Noise Trauma

Eight weeks after noise trauma, ABRs were again analyzed for possible signs of recovery. In all groups exposed to noise trauma at 8 kHz, a permanent threshold shift was observed for two out of three test frequencies. Consistently, ABR thresholds at 14 kHz were still significantly increased, with a difference in the threshold compared with the values before the noise trauma of 8 ± 15 dB in Mongolian gerbils ($n = 10$), 8 ± 5 dB in rats ($n = 10$), and 10 ± 10 dB in mice ($n = 10$) in the t8-group (Fig. 5*A*). Furthermore, ABR thresholds at 8 kHz (trauma frequency) were slightly increased. This increase, however, was significant in gerbils and rats. Moreover, mice in the t8-group also showed increased ABR thresholds at 2 kHz, a frequency that had not been affected directly after noise trauma. Therefore, other processes, such as aging, might also be involved. Rather unexpectedly, we did not detect significant increases in ABR thresholds at 16 kHz and 32 kHz in the t16-group of mice (noise trauma at 16 kHz). ABR waveforms and gain values at higher stimulus levels recovered to pretrauma values in all groups (Fig. 5, *B* and *C*). The variability in the gain factor (relating early to late ABR components) was highest in gerbils and lowest in mice (both the t8-group and t16-group). We assessed differences between males and females, and all male gerbils showed a reduced gain at 8 kHz stimulation (from 3.2 ± 1.1 to 1.5 ± 0.8), whereas all female gerbils showed an increased gain (from

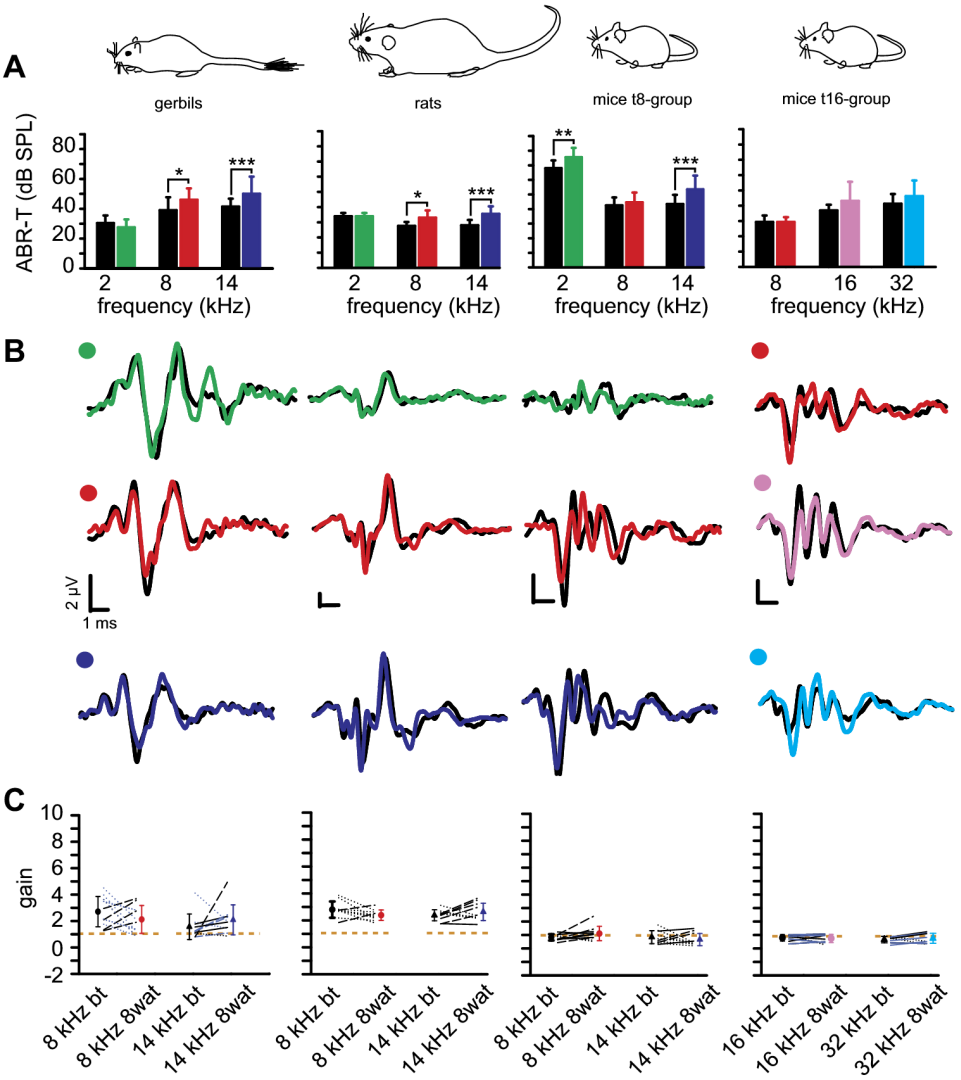

Figure 5. Recovery of hearing 8 wk after noise trauma in gerbils, rats, and mice. *A*: comparison of auditory brainstem response (ABR) threshold (ABR-T) levels before (black bars) and 8 wk after noise trauma (colored bars). ABR thresholds were determined at stimulus frequencies of 2 kHz (green bar), 8 kHz (red bar), and 14 kHz (dark blue bar) for gerbils (*left* column), rats (*second left* column), and mice exposed to trauma at 8 kHz (t8-group of mice, *second right* column). Although the standard noise trauma was set to 8 kHz, an additional mouse group (t16-group of mice, *right* column) experienced noise trauma at 16 kHz (pink bar) and was tested for changes in ABR threshold levels up to 32 kHz (light blue bar). *B*: comparison of average ABR waveforms at three stimulus frequencies before (black line) and 8 wk after noise trauma (colored lines, frequency color-coded as in *A*) recorded at a stimulus level of 80 dB sound pressure level (SPL). *C*: noise trauma-induced changes in the early-to-late amplitude gain of ABR peak components at 80 dB SPL. Lines indicate the direction of individual changes in gain before trauma (bt) and 8 wk after trauma (8 wat; increase: dashed line, stable/no change in gain: solid line, decrease in gain: dotted line). Individual data from males (gerbils and the t16-group of mice) are shown in blue, and data from females are shown in black. The horizontal dashed line indicates a gain of 1 (equal amplitude of early and late ABR components). Significant changes in thresholds over time for a particular species and frequency are indicated by $*P < 0.05$, $**P < 0.01$ and $***P < 0.001$.

1.9 ± 0.8 to 2.9 ± 0.8). A subsequent statistical analysis of sex-related differences was not possible due to the small group size (males: $n = 6$ and females: $n = 4$). In gerbils at higher frequencies of 14 kHz and in the t16-group of mice with mixed sexes, no trend for sex-specific differences in gain was observed. Very low variability in gain factors and positive gain slope values were prominent characteristics in the t16-group of mice, with no indications of sex-specific differences (Fig. 5*C*).

DISCUSSION

A comparison of auditory response measurements before, during, and up to 8 wk after consistent trauma induction revealed unexpected differences in the patterns of temporary and permanent hearing loss between the three rodent species. The time course of trauma development, especially during the two-step trauma induction, was consistent in all three species at frequencies higher than noise trauma. Differences were also observed; however, rats exhibited a substantial increase in the ABR threshold, with an even more surprising second reduction in sensitivity after an increase in the noise SPL by 10 dB.

In detail, we documented various effects of noise trauma on the processing of auditory signals in different rodent species. A key finding was the independence of ABR thresholds after acute noise trauma from baseline ABR thresholds in gerbils: across individuals, we detected the same level of threshold shift (see Fig. 4*B*, gerbil data). Moreover, we identified an upper limit of the ABR threshold shift directly after noise trauma. This hypothesis is based on the finding that neuronal activity at low levels (used to define ABR thresholds) depends on outer and inner hair cell-induced activity of afferent fibers that are sensitive to low level intensities and have high spontaneous firing rates (23, 44). The activity of these fibers mainly depends on the amplification process of outer hair cell motility, which is substantially affected by noise trauma due to outer hair cell damage (45). In rats and mice, noise trauma presumably leads to hair cell dysfunction and subsequent loss of these fibers, as indicated by shifts in the ABR threshold. Distinct differences in threshold shifts between animal groups suggest a species-specific susceptibility to noise damage. Unlike gerbils, threshold shifts in rats and mice depended on the individual hearing sensitivity before noise trauma: the lower the baseline hearing threshold was, the higher the amount of threshold shift after exposure. The absence of this correlation in gerbils raises questions about the sensitivity of specific hair cell structures, such as hair bundles or synaptic ribbons, to damage. This damage can be triggered by noise-induced inactivation of outer hair cell amplification (46). Our study indicates that typically observed traumatic damage/injuries, such as hair cell dysfunction and possible fiber loss (44), already occur during the first 30 min of exposure to high-level noise. Significant increases in the ABR threshold occurred within this time frame in all tested species after the onset of exposure to both noise trauma intensities.

Using ABR measurements, we calculated the gain between early and late ABR amplitude response components. For each animal, peak-to-peak amplitudes of late responses were divided by early responses. Although gerbils exhibited substantial variation in the extent of change in the gain after noise trauma, no general group trend was observed, as detected for rats and mice. This finding might be a reason to use gerbils in noise trauma studies since this animal model reflects the extent of heterogeneity observed in the human population. A more uniform response, on the other hand, would be advantageous for animal models to study the basic underlying mechanisms of hearing pathologies.

In mice, the gain factor increased from 0.8 to ~2 directly after trauma, representing a more than twofold increase in amplitude between early and late ABR responses. For both test groups of mice, this noise-induced increase in gain along the auditory pathway was observed at the center frequency of the noise trauma. Compensatory plasticity along the auditory pathway might account for this increase, as previously described for noise-exposed mice (47). In contrast to mice, a decrease in the gain factor after trauma compared with baseline was observed in rats. Thus, compensation for trauma-related changes at a higher neuronal level does not seem to occur in rats. However, a decrease in central gain was identified as a correlate of tinnitus in rats after noise trauma (4, 6). The striking species specificity might partly be explained by pigmentation. We used albino rats, while mice and gerbils were pigmented. An effect of pigmentation on hearing and otoprotection has already been documented in gerbils (48), rats (49), and guinea pigs (50), with albino animals having a more sensitive sense of hearing. Therefore, pigmentation might explain species-specific differences in trauma-induced neuronal compensation.

Designing a comparative study of noise-induced hearing loss with different rodent species is challenging since multiple variables, such as differences in body size, pigmentation, anesthetics, circadian rhythm, and onset of hearing loss, can affect the data. Recent data indicate that sex is also an important factor (49, 51, 52), and future studies should be designed to include male and female test groups. Although our strain is currently often used in auditory research, researchers might refrain from using C57BL/6 mice since this strain is particularly susceptible to early hair cell loss (38) and early onset of age-related hearing loss (53). A permanent increase in the threshold after noise trauma was present in all rodent groups with a noise center frequency of 8 kHz. The use of similar experimental conditions is an important factor contributing to the generation of such consistent effects. One component might be to apply noise trauma at a similar time of day because of the effect of circadian rhythms on threshold recovery (54, 55). A significant increase in the ABR threshold at 2 kHz in the t8-group of mice can be interpreted as an age-dependent effect, since an increase in the threshold of ~10 dB was found at low frequencies after ~24 wk in the BL6 mouse strain (56), which was the age of the mice at the end of the current study. Mice in the t16-group were 4 wk younger and did not show this hearing loss.

Taken together, the comparative approach revealed species-specific differences in the effectiveness and time course of trauma induction, as revealed by the ABR. Combined with the differential dependence on the hearing threshold, this result suggests that a variety of underlying mechanisms is involved in both sensitivity to traumatizing noise and recovery of hearing. Therefore, research focused on more than

just one animal model might provide greater benefits in the long run.

ACKNOWLEDGMENTS

The authors thank Steven Abendroth for providing technical support and Manfred Kössl for participating in helpful scientific discussion of the results and paper.

GRANTS

This work was supported by the Deutsche Forschungsgemeinschaft (DFG) through Grants NO 841/4-1 and 11-1 and GA 686/3-1.

DISCLOSURES

No conflicts of interest, financial or otherwise, are declared by the authors.

AUTHOR CONTRIBUTIONS

B.H.G. and M.N. conceived and designed research; L.K. performed experiments; L.K. and M.M.-D. analyzed data; L.K., B.H.G., and M.N. interpreted results of experiments; L.K. and M.N. prepared figures; L.K. and M.N. drafted manuscript; L.K., L.K., B.H.G., and M.N. edited and revised manuscript; L.K., L.K., M.M.-D., B.H.G., and M.N. approved final version of manuscript.

REFERENCES

1. **Le TN**, **Straatman LV**, **Lea J**, **Westerberg B.** Current insights in noise-induced hearing loss: a literature review of the underlying mechanism, pathophysiology, asymmetry, and management options. *J Otolaryngol Head Neck Surg* 46: 41, 2017. doi:10.1186/s40463-017-0219-x.
2. **Kujawa S**, **Liberman M.** Adding insult to injury: cochlear nerve degeneration after "temporary" noise-induced hearing loss. *J Neurosci* 29: 14077–14085, 2009. doi:10.1523/JNEUROSCI.2845-09.2009.
3. **Mannström P**, **Kirkegaard M**, **Ulfendahl M.** Repeated moderate noise exposure in the rat—an early adulthood noise exposure model. *J Assoc Res Otolaryngol* 16: 763–772, 2015. doi:10.1007/s10162-015-0537-5.
4. **Möhrle D**, **Hofmeier B**, **Amend M**, **Wolpert S**, **Ni K**, **Bing D**, **Klose U**, **Pichler B**, **Knipper M**, **Rüttiger L.** Enhanced central neural gain compensates acoustic trauma-induced cochlear impairment, but unlikely correlates with tinnitus and hyperacusis. *Neuroscience* 407: 146–169, 2019. doi:10.1016/j.neuroscience.2018.12.038.
5. **Zhang J**, **Song Y-L**, **Tian K-Y**, **Qiu J-H.** Minocycline attenuates noise-induced hearing loss in rats. *Neurosci Lett* 639: 31–35, 2017. doi:10.1016/j.neulet.2016.12.039.
6. **Koch L**, **Gaese BH**, **Nowotny M.** Strain comparison in rats differentiates strain-specific from more general correlates of noise-induced hearing loss and tinnitus. *J Assoc Res Otolaryngol* 23: 59–73, 2022. doi:10.1007/s10162-021-00822-2.
7. **Hockley A**, **Berger J**, **Palmer A**, **Wallace M.** Nitric oxide increases gain in the ventral cochlear nucleus of guinea pigs with tinnitus. *Eur J Neurosci* 52: 4057–4080, 2020. doi:10.1111/ejn.14913.
8. **Lin HW**, **Furman AC**, **Kujawa SG**, **Liberman MC.** Primary neural degeneration in the guinea pig cochlea after reversible noise-induced threshold shift. *J Assoc Res Otolaryngol* 12: 605–616, 2011. doi:10.1007/s10162-011-0277-0.
9. **Richter C-P**, **Young H**, **Richter SV**, **Smith-Bronstein V**, **Stock SR**, **Xiao X**, **Soriano C**, **Whitlon DS.** Fluvastatin protects cochleae from damage by high-level noise. *Sci Rep* 8: 3033, 2018. doi:10.1038/s41598-018-21336-7.
10. **Heffner HE**, **Harrington IA.** Tinnitus in hamsters following exposure to intense sound. *Hear Res* 170: 83–95, 2002. doi:10.1016/s0378-5955(02)00343-x.
11. **Manzoor N**, **Gao Y**, **Licari F**, **Kaltenbach J.** Comparison and contrast of noise-induced hyperactivity in the dorsal cochlear nucleus and inferior colliculus. *Hear Res* 295: 114–123, 2013. doi:10.1016/j.heares.2012.04.003.
12. **Boettcher FA.** Auditory brain-stem response correlates of resistance to noise-induced hearing loss in Mongolian gerbils. *J Acoust Soc Am* 94: 3207–3214, 1993. doi:10.1121/1.407226.
13. **Kiefer L**, **Schauen A**, **Abendroth S**, **Gaese B**, **Nowotny M.** Variation in acoustic overstimulation changes tinnitus characteristics. *Neuroscience* 310: 176–187, 2015. doi:10.1016/j.neuroscience.2015.09.023.
14. **Tziridis K**, **Ahlf S**, **Jeschke M**, **Happel MFK**, **Ohl FW**, **Schulze H.** Noise trauma induced neural plasticity throughout the auditory system of Mongolian gerbils: differences between tinnitus developing and non-developing animals. *Front Neurol* 6: 22, 2015. doi:10.3389/fneur.2015.00022.
15. **Chen T-J**, **Chen S-S.** Brain stem auditory-evoked potentials in different strains of rodents. *Acta Physiol Scand* 138: 529–538, 1990. doi:10.1111/j.1748-1716.1990.tb08881.x.
16. **Jewett DL**, **Romano MN.** Neonatal development of auditory system potentials averaged from the scalp of rat and cat. *Brain Res* 36: 101–115, 1972. doi:10.1016/0006-8993(72)90769-x.
17. **Melcher JR**, **Guinan JJ**, **Knudson IM**, **Kiang NYS.** Generators of the brainstem auditory evoked potential in cat. II. Correlating lesion sites with waveform changes. *Hear Res* 93: 28–51, 1996. doi:10.1016/0378-5955(95)00179-4.
18. **Land R**, **Burghard A**, **Kral A.** The contribution of inferior colliculus activity to the auditory brainstem response (ABR) in mice. *Hear Res* 341: 109–118, 2016. doi:10.1016/j.heares.2016.08.008.
19. **Kujawa S.** Noise-induced hearing loss. In: *Ballenger's Otorhinolaryngology: Head and Neck Surgery*, edited by Snow JB, Wackym PA. Hamilton, Ontario, Canada: BC Decker, 2003, p. 265–272.
20. **Eddins AC**, **Zuskov M**, **Salvi RJ.** Changes in distortion product otoacoustic emissions during prolonged noise exposure. *Hear Res* 127: 119–128, 1999. doi:10.1016/s0378-5955(98)00182-8.
21. **Singer W**, **Kasini K**, **Manthey M**, **Eckert P**, **Armbruster P**, **Vogt M**, **Jaumann M**, **Dotta M**, **Yamahara K**, **Harasztosi C**, **Zimmermann U**, **Knipper M**, **Rüttiger L.** The glucocorticoid antagonist mifepristone attenuates sound-induced long-term deficits in auditory nerve response and central auditory processing in female rats. *FASEB J* 32: 3005–3019, 2018. doi:10.1096/fj.201701041RRR.
22. **Valero MD**, **Burton JA**, **Hauser SN**, **Hackett TA**, **Ramachandran R**, **Liberman MC.** Noise-induced cochlear synaptopathy in rhesus monkeys (*Macaca mulatta*). *Hear Res* 353: 213–223, 2017. doi:10.1016/j.heares.2017.07.003.
23. **Furman AC**, **Kujawa SG**, **Liberman MC.** Noise-induced cochlear neuropathy is selective for fibers with low spontaneous rates. *J Neurophysiol* 110: 577–586, 2013. doi:10.1152/jn.00164.2013.
24. **Schaette R**, **McAlpine D.** Tinnitus with a normal audiogram: physiological evidence for hidden hearing loss and computational model. *J Neurosci* 31: 13452–13457, 2011. doi:10.1523/JNEUROSCI.2156-11.2011.
25. **Nowotny M**, **Kiefer L**, **Andre D**, **Fabrizius A**, **Hankeln T**, **Reuss S.** Hearing without neuroglobin. *Neuroscience* 366: 138–148, 2017. doi:10.1016/j.neuroscience.2017.10.010.
26. **Wang Y**, **Ren C.** Effects of repeated "benign" noise exposures in young CBA mice: shedding light on age-related hearing loss. *J Assoc Res Otolaryngol* 13: 505–515, 2012. doi:10.1007/s10162-012-0329-0.
27. **Wan G**, **Corfas G.** Transient auditory nerve demyelination as a new mechanism for hidden hearing loss. *Nat Commun* 8: 14487, 2017. doi:10.1038/ncomms14487.
28. **Liberman MC**, **Epstein MJ**, **Cleveland SS**, **Wang H**, **Maison SF.** Toward a differential diagnosis of hidden hearing loss in humans. *PLoS One* 11: e0162726, 2016. doi:10.1371/journal.pone.0162726.
29. **Plack CJ**, **Léger A**, **Prendergast G**, **Kluk K**, **Guest H**, **Munro KJ.** Toward a diagnostic test for hidden hearing loss. *Trends Hear* 20: 233121651665746, 2016. doi:10.1177/2331216516657466.
30. **Møller AR**, **Jannetta J.** Neural generators of the auditory brainstem response. In: *The Auditory Brainstem Response*, edited by Jacobson JT. San Diego, CA: College Hill Press, 1985, p. 13–32.
31. **Resnik J**, **Polley DB.** Cochlear neural degeneration disrupts hearing in background noise by increasing auditory cortex internal noise. *Neuron* 109: 984–996.e4, 2021. doi:10.1016/j.neuron.2021.01.015.
32. **Sturm JJ**, **Zhang-Hooks Y-X**, **Roos H**, **Nguyen T**, **Kandler K.** Noise trauma-induced behavioral gap detection deficits correlate with reorganization of excitatory and inhibitory local circuits in the inferior

colliculus and are prevented by acoustic enrichment. *J Neurosci* 37: 6314–6330, 2017. doi:10.1523/JNEUROSCI.0602-17.2017.
33. **Ohlemiller KK**, **Jones SM**, **Johnson KR.** Application of mouse models to research in hearing and balance. *J Assoc Res Otolaryngol* 17: 493–523, 2016. doi:10.1007/s10162-016-0589-1.
34. **Harding GW**, **Bohne BA**, **Vos JD.** The effect of an age-related hearing loss gene (Ahl) on noise-induced hearing loss and cochlear damage from low-frequency noise. *Hear Res* 204: 90–100, 2005. doi:10.1016/j.heares.2005.01.004.
35. **Hultcrantz M**, **Li HS.** Inner ear morphology in CBA/Ca and C57BL/6J mice in relationship to noise, age and phenotype. *Eur Arch Otorhinolaryngol* 250: 257–264, 1993. doi:10.1007/BF00186222.
36. **Li H-S**, **Borg E.** Age-related loss of auditory sensitivity in two mouse genotypes. *Acta Otolaryngol* 111: 827–834, 1991. doi:10.3109/00016489109138418.
37. **Liu H**, **Li G**, **Lu J**, **Gao Y-G**, **Song L**, **Li G-L**, **Wu H.** Cellular differences in the cochlea of CBA and B6 mice may underlie their difference in susceptibility to hearing loss. *Front Cell Neurosci* 13: 60, 2019. doi:10.3389/fncel.2019.00060.
38. **Spongr VP**, **Flood DG**, **Frisina RD**, **Salvi RJ.** Quantitative measures of hair cell loss in CBA and C57BL/6 mice throughout their life spans. *J Acoust Soc Am* 101: 3546–3553, 1997. doi:10.1121/1.418315.
39. **Li HS.** Genetic influences on susceptibility of the auditory system to aging and environmental factors. *Scand Audiol Suppl* 36: 1–39, 1992.
40. **Myint A**, **White CH**, **Ohmen JD**, **Li X**, **Wang J**, **Lavinsky J**, **Salehi P**, **Crow AL**, **Ohyam T**, **Friedman RA.** Large-scale phenotyping of noise-induced hearing loss in 100 strains of mice. *Hear Res* 332: 113–120, 2016. doi:10.1016/j.heares.2015.12.006.
41. **Valentinuzzi VS**, **Scarbrough K**, **Takahashi JS**, **Turek FW.** Effects of aging on the circadian rhythm of wheel-running activity in C57BL/6 mice. *Am J Physiol Regul Integr Comp Physiol* 273: R1957–R1964, 1997. doi:10.1152/ajpregu.1997.273.6.R1957.
42. **Harrison RT**, **Bielefeld EC.** Little evidence for a chronotolerance effect for impulse noise exposure in the C57BL/6J mouse. *Neurosci Lett* 684: 127–131, 2018. doi:10.1016/j.neulet.2018.07.028.
43. **Mehraei G**, **Hickox AE**, **Bharadwaj HM**, **Goldberg H**, **Verhulst S**, **Liberman MC**, **Shinn-Cunningham BG.** Auditory brainstem response latency in noise as a marker of cochlear synaptopathy. *J Neurosci* 36: 3755–3764, 2016. doi:10.1523/JNEUROSCI.4460-15.2016.
44. **Kujawa SG**, **Liberman MC.** Synaptopathy in the noise-exposed and aging cochlea: Primary neural degeneration in acquired sensorineural hearing loss. *Hear Res* 330: 191–199, 2015. doi:10.1016/j.heares.2015.02.009.
45. **Chen Y-S**, **Liu T-C**, **Cheng C-H**, **Yeh T-H**, **Lee S-Y**, **Hsu C-J.** Changes of hair cell stereocilia and threshold shift after acoustic trauma in guinea pigs: comparison between inner and outer hair cells. *ORL J Otorhinolaryngol Relat Spec* 65: 266–274, 2003. doi:10.1159/000075224.
46. **Chen G-D.** Prestin gene expression in the rat cochlea following intense noise exposure. *Hear Res* 222: 54–61, 2006. doi:10.1016/j.heares.2006.08.011.
47. **Schrode KM**, **Muniak MA**, **Kim Y-H**, **Lauer AM.** Central compensation in auditory brainstem after damaging noise exposure. *eNeuro* 5: ENEURO.0250-18.2018, 2018. doi:10.1523/ENEURO.0250-18.2018.
48. **Szymanski MD**, **Henry KR**, **Buchting FO.** Albino and pigmented gerbil auditory function: influence of genotype and gentamicin. *Audiology* 33: 63–72, 1994. doi:10.3109/00206099409071868.
49. **Overbeck GW**, **Church MW.** Effects of tone burst frequency and intensity on the auditory brainstem response (ABR) from albino and pigmented rats. *Hear Res* 59: 129–137, 1992. doi:10.1016/0378-5955(92)90110-9.
50. **Conlee JW**, **Abdul-Baqi KJ**, **McCandless GA**, **Creel DJ.** Differential susceptibility to noise-induced permanent threshold shift between albino and pigmented guinea pigs. *Hear Res* 23: 81–91, 1986. doi:10.1016/0378-5955(86)90177-2.
51. **Lin N**, **Urata S**, **Cooka R**, **Makishima T.** Sex differences in the auditory functions of rodents. *Hear Res* 7: 108271, 2021. doi:10.1016/j.heares.2021.108271.
52. **Milon B**, **Mitra S**, **Song Y**, **Margulies Z**, **Casserly R**, **Drake V**, **Mong JA**, **Depireux DA**, **Hertzano R.** The impact of biological sex on the response to noise and otoprotective therapies against acoustic injury in mice. *Biol Sex Differ* 9: 9–12, 2018. doi:10.1186/s13293-018-0171-0.
53. **Scimemi P**, **Santarelli R**, **Selmo A**, **Mammano F.** Auditory brainstem responses to clicks and tone bursts in C57 BL/6J mice. *Acta Otorhinolaryngol Ital* 34: 264–271, 2014.
54. **Basinou V**, **Park J**, **Cederroth C**, **Canlon B.** Circadian regulation of auditory function. *Hear Res* 347: 47–55, 2017. doi:10.1016/j.heares.2016.08.018.
55. **Cederroth CR**, **Park J**, **Basinou V**, **Weger BD**, **Tserga E**, **Sarlus H**, **Magnusson AK**, **Kadri N**, **Gachon F**, **Canlon B.** Circadian regulation of cochlear sensitivity to noise by circulating glucocorticoids. *Curr Biol* 29: 2477–2487.e6, 2019. doi:10.1016/j.cub.2019.06.057.
56. **Ison JR**, **Allen PD**, **O'Neill WE.** Age-related hearing loss in C57BL/6J mice has both frequency-specific and non-frequency-specific components that produce a hyperacusis-like exaggeration of the acoustic startle reflex. *J Assoc Res Otolaryngol* 8: 539–550, 2007. doi:10.1007/s10162-007-0098-3.